



Volumetric, acoustic and spectroscopic approaches to understand the molecular interactions between 1-butyl-3-methylimidazolium hexafluorophosphate and *N*-vinyl-2-pyrrolidinone

P. Suneetha¹ · T. S. Krishna² · M. Gowrisankar³ · M. Srinivasa Reddy⁴ · D. Ramachandran¹

Received: 22 August 2017 / Accepted: 27 May 2018
© Akadémiai Kiadó, Budapest, Hungary 2018

Abstract

In the present paper, we reported the accurately measured densities (ρ), speed of sound (u) and refractive index (n_D) for the binary mixture of 1-butyl-3-methylimidazolium hexafluorophosphate [Bmim] [PF₆] with *N*-vinyl-2-pyrrolidinone (NVP) as a function of concentration at six temperatures from 298.15 to 323.15 K at atmospheric pressure. From the measured density, speed of sound and refractive index, the excess molar volumes, V_m^E , excess isentropic compressibilities, κ_s^E , excess speeds of sound, u^E , excess molar isentropic compressibility, $K_{s,m}^E$, deviation in refractive index, $\Delta_\phi n_D$ and deviation in molar refraction, ΔR_M have been calculated and satisfactorily fitted using the Redlich–Kister polynomial equation. Partial molar volumes and molar isentropic compressibilities were calculated. Infinite dilution values of these derived thermodynamic properties have also been calculated. Evaluation of refractive index has been carried out by nine mixing rules, to investigate their validity for these mixtures over the entire mole fraction of [Bmim][PF₆] at all investigated temperatures. Comparison of these approaches has been presented in terms of APD. Furthermore, the FTIR measurements of these mixtures are carried out at 298.15 K to study the complex formation between [Bmim][PF₆] and NVP. Changes in the measured and calculated values of the physicochemical parameters as a function of temperature and composition of the mixture were analysed in terms of interactions. The results were used to quantitatively analyse the effects of organic solvent NVP with [Bmim] [PF₆] and compared with other anions of [Bmim].

Keywords 1-Butyl-3-methylimidazolium hexafluorophosphate [Bmim] [PF₆] · *N*-Vinyl-2-pyrrolidinone (NVP) · Excess properties · FTIR spectroscopy

Electronic supplementary material The online version of this article (<https://doi.org/10.1007/s10973-018-7427-0>) contains supplementary material, which is available to authorized users.

✉ T. S. Krishna
sritadikonda@gmail.com

✉ D. Ramachandran
dittakavirc@gmail.com

¹ Department of Chemistry, Acharya Nagarjuna University, Nagarjuna Nagar, Guntur, Andhra Pradesh 522510, India

² Department of Physics, A.S.N. Women's Engineering College, Tenali, Andhra Pradesh 522201, India

Introduction

New methods of laboratory work as well as new technologies increasingly require the use of solvents with desired properties. The solution may be the use of multi-component liquid mixtures instead of pure solvents. Physicochemical properties of such systems significantly differ from the properties of their pure components, and

³ Department of Chemistry, J.K.C.C. Acharya Nagarjuna University, Guntur, Andhra Pradesh 522006, India

⁴ Department of Chemistry, T.R.R. Government Degree College, Kandukur, Andhra Pradesh 523105, India

their thorough studies provide information not only about the interactions occurring in such systems, but also allow wider application of the investigated mixtures in practice [1]. The authors also show how one can get a lot of thermodynamic data only from the density measurements without the use of complicated and labour-intensive calorimetric methods.

The information of thermo- and physicochemical behaviour of ILs is especially important to plan new inventories including ILs and industrial processes [2]. The ILs are occupying the place of volatile organic compounds because of their negligible vapour pressures. The ILs as recyclable solvents have prompt diminishment in VOC emanations and furthermore to a practical utilization of beginning materials in industry [3].

ILs are specially known as architect solvents in the light of the fact that their properties can be changed to specific applications with interesting mixtures of cations and anions [4]. Apart from changing the cations and anions, an addition of co-solvent to improve the physicochemical properties of these designer solvents is also gaining scientific attention to scientific researchers to discover their novel applications [5–7].

From past 10–15 years, scientists as well as chemists initiated action to address environmental issues in a safe and gainful manner under the name “green chemistry” to highlight the judicious use of chemistry for prevention of pollution through environmentally conscious designing of chemical processes. So, solvents play a wider role in analytical chemistry, product purification, extraction and separation technologies. Therefore, to make chemistry more sustainable in these fields, knowledge of alternative, greener solvents or their mixtures were important in order to replace traditional organic solvents.

There are some critical evaluation criteria for selecting novel working pairs such as to ensure high efficiency of absorption hydrodesulfurization (HDS) to be noncorrosive, to be nontoxic and to ensure secure operation and so on. The determination of the fitting ionic fluid and its capacity to extricate aromatic sulphur compounds is troublesome in these sorts of process. *N*-vinyl-2-pyrrolidinone is one of the particular advantages in decolorizing crude oil free from asphaltic constituents and as an adsorbent for sour gases from crude natural gas [8]. So, the combination mixture makes more advantage in petro-product extraction.

This work is a continuation of our comprehensive study [9, 10] related to the study of acoustic, volumetric and refractive index properties of binary mixtures of ionic liquids with volatile organic compound of *N*-vinyl-2-pyrrolidinone (NVP) with the enhancement of temperature at ambient pressure (0.1 MPa). In spite of importance of properties of ILs with NVP, there is limited information available on the thermodynamic properties of IL mixtures

with other fluids, and these properties are still lacking. The present study is therefore undertaken to evaluate the influence of particular specific interactions on the excess properties with the enhancement of temperature, and the presence of anion in the IL and the NVP.

In the present study, we report the densities, ρ , speeds of sound, u and refractive indices, n_D of binary mixtures of [Bmim][PF₆] and NVP, over the entire composition range at temperatures (298.15–323.15) K and at atmospheric pressure. Pure liquids data were taken from our previous papers [9, 11]. Using the experimental data, the excess and excess partial molar volumes of the components at infinite dilution have also been calculated. The variations of these parameters with composition and temperature have been discussed in terms of intermolecular interactions prevailing in these mixtures.

Experimental

Materials

The names, provenances and purities of the solutes used in this work are given in Table 1. The 1-butyl-3-methylimidazolium hexafluorophosphate [Bmim][PF₆] was procured from Iolitec (Germany); the mass fraction purity of the ionic liquids (as stated by the manufacturer) is > 0.99 with less than 100 ppm water content and less than 100 ppm halide ion concentration. In order to reduce the water content to negligible values, vacuum (0.1 Pa) and moderate temperature (60 °C) were applied to [Bmim][PF₆] for several days, prior to use. After drying under vacuum and 60 °C temperature, the water content was found to be within limits specified by the manufacturer (890 KF Titrand, Metrohm, USA) [12].

[BMIM][PF₆] purity was checked through ¹H-NMR on an advance DPX400 Bruker initial and after drying is shown in Figures 1S and 2S (*supplementary material*). NMR spectra are well matched with report conducted by Dupont et al. [13, 14] and utilized without further purification.

¹H NMR (CDCl₃): δ = 0.96 ppm (t, 3H, J = 7.21), δ = 1.29 ppm (m, 2H), δ = 1.78 ppm (m, 2H), δ = 3.83 ppm (s, 3H), δ = 4.09 ppm (t, 2H, J = 7.40), δ = 7.25 ppm (d, 1H, J = 3.51), δ = 7.30 ppm (d, 1H, J = 5.35), δ = 8.35 ppm (s, 1H).

In FTIR, three vibrational modes of water were detectable and did not increase much after exposure during a few hours to air. Water molecules were not hydrogen bonded to each other, as in this IL no band was detectable in the range of 3550–3250 cm⁻¹. All these findings are comparable to the existing literature [15]. The intensities of the IL bands did not decrease by more than 1

Table 1 Specification of chemical samples

Chemical name (CAS number)	Source	Initial mass fraction purity	Purification method	Final mass fraction purity	Analysis method	Water mass fraction (ppm)	Water analysis method
[Bmim][PF ₆] (174501-64-5)	Iolitech, Germany	> 0.995	Degassed under vacuum	> 0.995	NA	< 40	Karl Fischer
N-Vinyl-2-pyrrolidinone (88-12-0)	Sigma-Aldrich, India	> 0.97	Fractional distillation	> 0.98	GC ^a	< 150	Karl Fischer

^aGas chromatography

or 2%. Therefore, it was not possible to quantify the probable small swelling of [Bmim][PF₆] caused by the diffusion of water into the IL and found a good agreement with the literature [16].

NVP was procured from Sigma-Aldrich, USA, with mass fraction purity of 0.97 and was purified by the fractional distillation method under reduced pressure [17]. Purity was checked by gas chromatograph (GC), and water content of NVP was found less than 150 ppm [10]. The sample preparation was done as described in our previous publication [18]. The solutions were prepared by weighing with CPA-225D (Japan) electronic balance, sensitive to ± 0.01 mg. The uncertainty in the mole fraction was estimated to be within $\pm 1 \cdot 10^{-4}$. In order to avoid water absorption, the ionic liquid was used inside a glove box under argon. The scattered speed of sound values was graphically compared with George et al. [19], with our results in supplementary material, Figure 3S. In our opinion, the differences may be due to the measurement procedure such as ultrasonic interferometer (Mittal Enterprises, New Delhi, India) operated at a fixed frequency of 2 MHz and some of issues such as purity of the NVP (97%). The density of [Bmim][PF₆] was graphically compared with average absolute deviation ($AAD = (100/n) \sum_{i=1}^n |\rho_{lit}/\rho_{exp} - 1|$) in Fig. 1 with the literature [20–27] at $T = 298.15$ – 323.15 K which agrees with literature values with a maximum absolute deviation less than 0.25%.

Apparatus and procedure

Densities and speed of sound were measured by an Anton Paar DSA 5000 M, high-precision vibrating tube digital densimeter and speed of sound measuring device, with automatic viscosity corrections. The instrument has a built-in thermostat to maintain the temperature between 0 and 70 °C with a precision of ± 0.001 °C. Its piezo frequency is around 3 MHz. The densimeter was calibrated randomly with dry air at atmospheric pressure and triply distilled, freshly degassed and deionized water

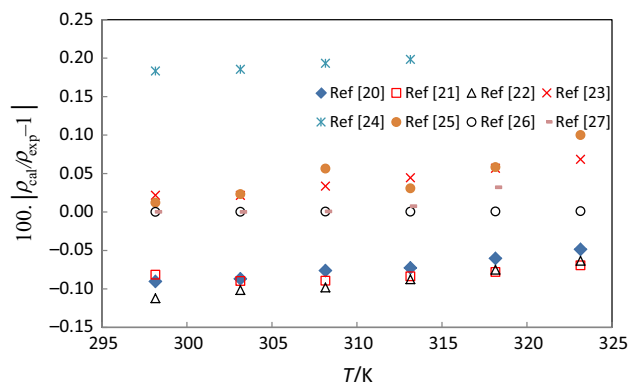


Fig. 1 Graphical comparison density of [Bmim][PF₆] with various researchers [20–27]

($\rho = 997.075$ kg m⁻³ at 298.15 K) supplied by Anton-Paar as described elsewhere. The standard uncertainties associated with the measurements for temperature, density and speed of sound were estimated to be within ± 0.01 K, ± 0.8 kg m⁻³ and ± 1 m s⁻¹, respectively [28]. A third-order polynomial was used to fit the speed of sound as a function of concentration (b_i), for pure substances and its binary mixture of [Bmim][PF₆] with NVP are listed in Table 1S and Fig 4S (*Supplementary material*).

The refractive indices of pure components and binary mixtures were measured with an automatic digital precision refractometer by Dr. Krenchen Abbemat HP (RXA170 Heavy duty, Anton Paar, Austria) as described elsewhere [29]. The uncertainties in the temperature and refractive index measurements were estimated to be within ± 0.02 K and ± 0.0005 , respectively.

FTIR measurements of pure [Bmim][PF₆], NVP and 0.1–0.9 mol fractions of [Bmim][PF₆] + NVP mixtures were carried out with FTIR Spectrometer (Alpha FTIR, Bruker, Germany) with accessory Alpha E by using ATR technique (400–4000) cm⁻¹ with 4.0 cm⁻¹ resolution to investigate the strength of molecular associations in these mixtures. All spectrums were recorded at room temperature. The IR data were analysed using OPUS 6.5 software.

Theory

Excess properties

To understand the molecular interactions of [Bmim][PF₆] + NVP the thermophysical properties such as density, ρ , speed of sound, u , and refractive index, n_D , were determined over the mole fraction range at temperature range from $T/K = 298.15$ – 323.15 , at atmospheric pressure and given in Table 2. Excess molar volume (V_m^E), excess isentropic compressibility (κ_s^E), excess molar isentropic compressibility ($K_{s,m}^E$), excess speed of sound (u^E) and deviation refractive index (Δn_D) were calculated from the experimental density, speed of sound and refractive index measurement by the relationships [30–32]:

$$V_m^E = V_m - V_m^{\text{id}} \quad (1)$$

$$\kappa_s^E = \kappa_s - \kappa_s^{\text{id}} \quad (2)$$

$$K_{s,m}^E = K_{s,m} - K_{s,m}^{\text{id}} \quad (3)$$

$$u^E = u - u^{\text{id}} \quad (4)$$

The thermodynamic properties of molar volume V_m , the coefficient of thermal expansion, α_p , and the isentropic compressibility, κ_s values are derived directly from the experimental measurements with density ρ , and speed of sound, u .

$$\alpha_p = -\frac{1}{\rho} \left(\frac{\Delta \rho}{\Delta T} \right)_p \quad (5)$$

In this work, α_p values are obtained from a linear dependence of ρ with T . The C_p values of the pure liquids at investigated temperatures have been taken from our previous papers [9, 20].

Excess isobaric thermal expansivity

To extend an understanding of the molecular interaction of the solution during mixing, excess isobaric thermal expansivity was calculated for the investigated composition [33], and to know more the difference between numerical (Eq. 5) and analytical methods (Eq. 6) [34] is of isobaric thermal expansion. For more clarity, authors calculated the excess thermal expansivity (α_p^E).

By analytically, α_p can be calculated as

$$\alpha_p = -\frac{1}{\rho} \left(\frac{\partial \rho}{\partial T} \right)_p \quad (6)$$

$$\alpha_p^E/(K^{-1}) = \alpha_p - \alpha_p^{\text{id}} = (\partial V_m / \partial T)_p / V_m - \sum_{i=1}^2 \phi_i \alpha_{p,i}^* \quad (7)$$

The deviation in refractive index, $\Delta_\phi n_D$, has been calculated on the basis of volume fraction [35] as

$$\Delta_\phi n_D = n_D - \left[\phi_1 (n_{D,1})^2 + \phi_2 (n_{D,2})^2 \right]^{1/2} \quad (8)$$

Molar refraction, R_M , was obtained from experimental refractive index data by using the following expression

$$R_M = \left[\frac{n_D^2 - 1}{n_D^2 + 2} \right] V_m$$

The deviation in molar refraction, ΔR_M , has been calculated by using the following expression [35]

$$\Delta R_M = R - (x_1 R_{M,1} + x_2 R_{M,2}) \quad (9)$$

The values of V_m^E , κ_s^E , $K_{s,m}^E$, u^E , ΔR_m as functions of mole fraction, x_1 of [Bmim][PF₆] and temperature for both the systems are presented in Table 3.

The excess values of the above parameters for the mixtures have been fitted to the Redlich–Kister [36] polynomial equation

$$Y^E = x_1 x_2 \sum_{i=1}^n A_i (2x_1 - 1)^i \quad (10)$$

where Y^E is V_m^E , κ_s^E , $K_{s,m}^E$ and u^E , $\Delta_\phi n_D$, ΔR_m and α_p^E . The equation coefficients, A_i , obtained by the method of least squares with equal weights assigned to each point were calculated along with the standard deviation $\sigma(Y^E)$. The coefficients were adjustable parameters for a better fit of the excess functions.

The standard deviation $\sigma(Y^E)$ is calculated using,

$$\sigma(Y^E) = \left(\frac{\sum (Y_{\text{expt}}^E - Y_{\text{cal}}^E)^2}{(m - n)} \right)^{1/2} \quad (11)$$

where m is equal to the number of experimental points, n is the number of A_i coefficients considered ($n + 1$ in the present study). The optimal number of A_i coefficients has been determined statistically by performing F -test. If the p value is small, we can accept the null hypothesis. Then only we can consider the F -value. In other words, p value and F -value should both be statistically significant in order to correctly interpret the results. The coefficients, A_i and corresponding standard deviations, σ fit of V_m^E , κ_s^E , $K_{s,m}^E$, u^E , $\Delta_\phi n_D$, ΔR_m , α_p^E , standard error, F -values and p values are given in Table 4. The variations of V_m^E , κ_s^E , $K_{s,m}^E$, u^E , $\Delta_\phi n_D$ and ΔR_m and α_p^E with mole fraction, x_1 , along with smoothed values from Eq. (10) at studied temperatures are shown graphically in Figs. 2, 4–7, 5S and 6S, respectively.

Table 2 Densities, ρ , speeds of sound, u , refractive index, n_D as a function of mole fraction, x_1 of [Bmim][PF₆] for [Bmim][PF₆] + NVP binary mixtures at the temperatures, $T = (298.15\text{--}323.15)$ K and at pressure $p = 0.1$ MPa

x_1	T/K					
	298.15	303.15	308.15	313.15	318.15	323.15
$\rho/(\text{kg m}^{-3})$						
0.0000 [8]	1039.4	1035.0	1030.6	1026.1	1021.7	1017.3
0.1011	1102.5	1098.2	1094.0	1089.7	1085.4	1081.1
0.2059	1156.1	1151.9	1147.7	1143.5	1139.2	1135.1
0.3019	1197.0	1192.8	1188.7	1184.5	1180.3	1176.2
0.3937	1230.3	1226.2	1222.0	1217.9	1213.7	1209.6
0.5023	1264.0	1259.9	1255.7	1251.6	1247.4	1243.3
0.5840	1286.0	1281.8	1277.6	1273.5	1269.3	1265.2
0.6946	1311.9	1307.8	1303.6	1299.4	1295.2	1291.0
0.7788	1329.3	1325.1	1320.9	1316.7	1312.5	1308.3
0.8707	1346.3	1342.1	1337.9	1333.6	1329.4	1325.2
1.0000 [10]	1367.2	1363.0	1358.7	1354.5	1350.2	1346.0
$u/(\text{m s}^{-1})$						
0.0000 [8]	1521.5	1502.5	1483.7	1465.0	1446.5	1428.1
0.1011	1515.9	1498.9	1481.8	1464.7	1447.8	1431.1
0.2059	1506.0	1490.1	1474.2	1458.3	1442.6	1427.0
0.3019	1496.4	1481.4	1466.3	1451.4	1436.6	1422.0
0.3937	1487.8	1473.5	1459.2	1444.9	1430.9	1416.9
0.5023	1477.6	1463.9	1450.2	1436.7	1423.4	1410.2
0.5840	1470.5	1457.4	1444.3	1431.2	1418.4	1405.7
0.6946	1461.5	1449.1	1436.4	1423.9	1411.6	1399.4
0.7788	1455.7	1443.4	1431.1	1419.0	1407.0	1395.1
0.8707	1449.9	1437.9	1425.8	1414.0	1402.3	1390.8
1.0000 [10]	1443.8	1431.7	1419.8	1408.2	1396.8	1385.6
n_D						
0.0000 [8]	1.5104	1.5081	1.5058	1.5035	1.5012	1.4989
0.1011	1.4953	1.4932	1.4910	1.4889	1.4868	1.4847
0.2059	1.4808	1.4788	1.4769	1.4749	1.4729	1.4710
0.3019	1.4686	1.4667	1.4649	1.4631	1.4612	1.4594
0.3937	1.4578	1.4561	1.4544	1.4526	1.4509	1.4492
0.5023	1.4463	1.4447	1.4430	1.4414	1.4398	1.4382
0.5840	1.4384	1.4369	1.4353	1.4338	1.4323	1.4307
0.6946	1.4290	1.4275	1.4260	1.4246	1.4231	1.4216
0.7788	1.4227	1.4213	1.4198	1.4184	1.4170	1.4155
0.8707	1.4166	1.4153	1.4139	1.4125	1.4111	1.4097
1.0000 [10]	1.4097	1.4084	1.4071	1.4057	1.4043	1.4029

Standard uncertainties s are $s(T) = \pm 0.01$ K, $s(x) = \pm 1.0 \times 10^{-4}$, $s(\rho) = \pm 0.8$ kg m⁻³, $s(u) = \pm 1$ m s⁻¹, $s(n_D) = \pm 0.0005$, $s(T)$ for n_D = ± 0.02 K, and $s(p) = \pm 1.0$ kPa

Partial molar properties

In addition to other volumetric properties (partial molar volumes and partial molar compressibility) $\bar{Y}_{m,1}$ and $\bar{Y}_{m,2}$ of IL and NVP over the entire concentration range in investigated system have been determined using the following equations

$$\bar{Y}_{m,1} = Y_s^E + Y_{m,1}^* + x_2 \left(\frac{\partial Y_s^E}{\partial x_1} \right)_{T,p} \quad (12)$$

$$\bar{Y}_{m,2} = Y_s^E + Y_{m,2}^* - x_1 \left(\frac{\partial Y_s^E}{\partial x_1} \right)_{T,p} \quad (13)$$

where Y is V or K_s where $Y_{m,1}^*$ and $Y_{m,2}^*$ are the molar components of pure components IL and NVP, respectively.

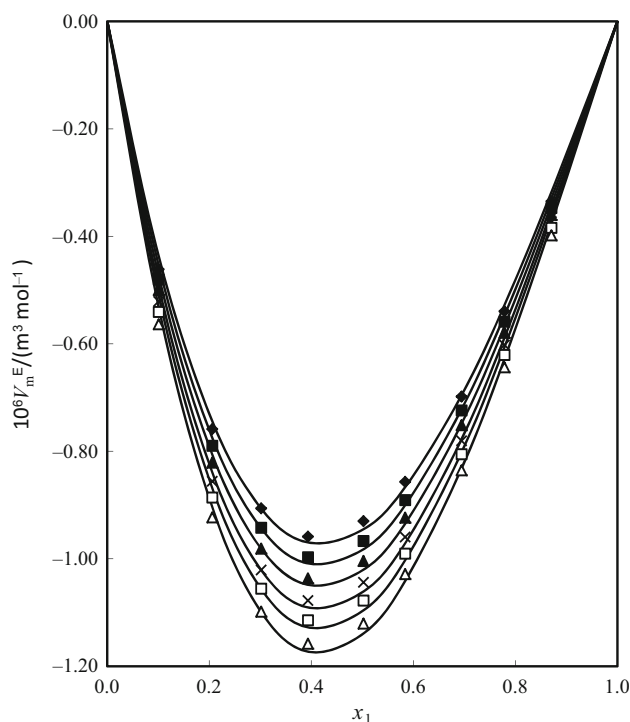


Fig. 2 Plots of excess molar volume, V_m^E versus mole fraction, x_1 of [Bmim][PF₆] for [Bmim][PF₆] + NVP binary mixtures at temperatures, $T/K = 298.15$, \blacklozenge ; At $T/K = 303.15$, \blacksquare ; $T/K = 308.15$, \blacktriangle ; $T/K = 313.15$, \times ; $T/K = 318.15$, \square ; $T/K = 323.15$, Δ . The points represent experimental values, and lines represent values calculated from Eq. (10) using the coefficients given in Table 4

The derivative $(\partial Y_s^E / \partial x_1)_{T,p}$ in Eqs. (12) and (13) was obtained by differentiation, which lead to the following equations for $\bar{Y}_{m,1}$ and $\bar{Y}_{m,2}$.

$$\bar{Y}_{m,1} = \bar{Y}_{m,1}^* + x_2^2 \sum_{i=0}^j A_i (1 - 2x_1)^i - 2x_1 x_2^2 \sum_{i=0}^j A_i (1 - 2x_1)^{i-1} \quad (14)$$

$$\bar{Y}_{m,2} = \bar{Y}_{m,2}^* + x_1^2 \sum_{i=0}^j A_i (1 - 2x_1)^i + 2x_2 x_1^2 \sum_{i=0}^j A_i (1 - 2x_1)^{i-1} \quad (15)$$

$Y_{m,1}^*$ and $Y_{m,2}^*$ are the molar properties of pure components, and the excess partial molar properties are calculated by the following relations [37, 38],

$$\bar{Y}_{m,i}^E = Y_m^E + (1 - x_1) \left(\frac{\partial Y_m^E}{\partial x_1} \right) \quad (16)$$

We are interested to evaluate the partial molar properties of [Bmim][PF₆] at infinite dilution ($x_1 = 0$) in NVP, and the partial molar properties of NVP at infinite dilution ($x_2 = 0$)

in [Bmim][PF₆]. Therefore, $\bar{Y}_{m,1}^\circ$ is obtained by setting $x_1 = 0$ which leads to

$$\bar{Y}_{m,1}^\circ = Y_{m,1}^* + \sum_{i=0}^n A_i (-1)^i \quad (17)$$

Similarly, setting $x_2 = 0$ leads to

$$\bar{Y}_{m,2}^\circ = Y_{m,2}^* + \sum_{i=0}^n A_i \quad (18)$$

here $\bar{Y}_{m,1}^\circ$ and $\bar{Y}_{m,2}^\circ$ represent the partial molar properties of [Bmim][PF₆] at infinite dilution in NVP and the partial molar properties of NVP at infinite dilution in [Bmim][PF₆], respectively.

Excess partial molar properties at infinite dilution $\bar{Y}_{m,i}^{\circ,E}$ for each component in binary liquid mixtures are evaluated through relations

$$\bar{Y}_{m,1}^{\circ,E} = \bar{Y}_{m,1}^\circ - Y_{m,1}^* \quad (19)$$

$$\bar{Y}_{m,2}^{\circ,E} = \bar{Y}_{m,2}^\circ - Y_{m,2}^* \quad (20)$$

The variations of $\bar{V}_{m,1}^E$ and $\bar{V}_{m,2}^E$; and $\bar{K}_{s,m,1}^E$ and $\bar{K}_{s,m,2}^E$ with composition and temperature are listed in Tables 3S–4S as given in *supplementary material* and are presented graphically in Figs. 8 and 9, respectively.

The values of partial molar properties, $\bar{Y}_{m,1}^\circ$ and $\bar{Y}_{m,2}^\circ$, of [Bmim][PF₆] and NVP at infinite dilution are calculated by using Eqs. (17)–(18), and the excess partial molar properties, $\bar{Y}_{m,1}^{\circ,E}$ and $\bar{Y}_{m,2}^{\circ,E}$ at infinite dilution are calculated using Eqs. (19) and (20). The values of $\bar{V}_{m,1}^\circ$, $V_{m,1}^*$, $\bar{V}_{m,1}^{\circ,E}$, $\bar{V}_{m,2}^\circ$, $V_{m,2}^*$ and $\bar{V}_{m,2}^{\circ,E}$; and $\bar{K}_{s,m,1}^\circ$, $K_{s,m,1}^*$, $\bar{K}_{s,m,1}^{\circ,E}$, $\bar{K}_{s,m,2}^\circ$, $K_{s,m,2}^*$ and $\bar{K}_{s,m,2}^{\circ,E}$ for the binary mixtures at each investigated temperature are listed in Tables 5 and 6, respectively.

Results and discussion

Excess properties

The experimental values of densities (ρ), speed of sound (u), refractive index (n_D) were used to calculate excess properties such as excess molar volume (V_m^E), isentropic compressibility (κ_s^E), excess molar isentropic compressibility ($K_{s,m}^E$), excess speed of sound (u^E), deviation in refractive index $\Delta_\phi n_D$, and deviations in molar refractive index (ΔR_m) of the binary mixtures over the entire composition range and at 298.15–323.15 K temperatures are listed in Table 2. The variation of pure values of ρ , u and n_D with temperature is found to be linear, whereas variation of ρ , u and n_D with mole fraction is found to be nonlinear.

Table 3 Excess molar volume (V_m^E), excess isentropic compressibility (κ_s^E), excess molar isentropic compressibility ($K_{s,m}^E$), excess speed of sound (u^E), deviation in refractive index ($\Delta_\phi n_D$), deviation in molar refraction (ΔR_M) and excess isobaric expansivity (α_p^E) as a function of mole fraction, x_1 of [Bmim][PF₆] for [Bmim][PF₆] + NVP at the temperatures $T = (298.15\text{--}323.15)$ K at pressure $p = 0.1$ MPa

x_1	V_m^E $10^6/\text{m}^3 \text{ mol}^{-1}$	κ_s^E $10^{10}/\text{m}^2 \text{ N}^{-1}$	$K_{s,m}^E$ $10^{14}/\text{m}^5 \text{ N}^{-1} \text{ mol}^{-1}$	u^E $10^{-2}/\text{m s}^{-1}$	$10^6 \cdot \Delta R_M/\text{m}^3 \text{ mol}^{-1}$	$10^2 \cdot \Delta_\phi n_D$	$\alpha_p^E/\text{kK}^{-1}$
298.15 K							
0.1011	-0.461	-0.109	-0.141	0.174	0.071	-0.117	-2.137
0.2059	-0.759	-0.159	-0.224	0.259	0.104	-0.442	-3.886
0.3019	-0.906	-0.170	-0.260	0.282	0.102	-0.639	-5.045
0.3937	-0.959	-0.163	-0.266	0.272	0.076	-0.540	-5.745
0.5023	-0.930	-0.139	-0.246	0.233	0.025	-0.708	-6.047
0.5840	-0.857	-0.116	-0.217	0.194	-0.019	-0.440	-5.893
0.6946	-0.698	-0.081	-0.163	0.134	-0.070	-0.596	-5.162
0.7788	-0.540	-0.054	-0.116	0.089	-0.092	-0.492	-4.200
0.8707	-0.335	-0.028	-0.065	0.045	-0.086	-0.196	-2.750
303.15 K							
0.1011	-0.481	-0.115	-0.150	0.178	0.064	-0.115	-2.204
0.2059	-0.790	-0.169	-0.240	0.266	0.095	-0.434	-4.012
0.3019	-0.942	-0.182	-0.278	0.291	0.092	-0.629	-5.216
0.3937	-0.997	-0.174	-0.286	0.282	0.066	-0.530	-5.945
0.5023	-0.967	-0.150	-0.265	0.244	0.016	-0.696	-6.263
0.5840	-0.891	-0.125	-0.234	0.203	-0.026	-0.431	-6.108
0.6946	-0.724	-0.088	-0.177	0.142	-0.074	-0.586	-5.354
0.7788	-0.559	-0.060	-0.127	0.096	-0.094	-0.484	-4.359
0.8707	-0.347	-0.031	-0.072	0.049	-0.087	-0.192	-2.855
308.15 K							
0.1011	-0.500	-0.122	-0.160	0.182	0.059	-0.110	-2.273
0.2059	-0.821	-0.179	-0.256	0.273	0.087	-0.424	-4.143
0.3019	-0.981	-0.194	-0.297	0.299	0.083	-0.616	-5.392
0.3937	-1.037	-0.186	-0.305	0.290	0.058	-0.516	-6.151
0.5023	-1.004	-0.160	-0.284	0.252	0.011	-0.681	-6.485
0.5840	-0.924	-0.134	-0.251	0.211	-0.029	-0.419	-6.328
0.6946	-0.751	-0.094	-0.191	0.149	-0.076	-0.573	-5.550
0.7788	-0.580	-0.064	-0.137	0.100	-0.094	-0.473	-4.520
0.8707	-0.360	-0.034	-0.077	0.052	-0.086	-0.186	-2.961
313.15 K							
0.1011	-0.521	-0.129	-0.170	0.184	0.054	-0.105	-2.345
0.2059	-0.856	-0.190	-0.271	0.277	0.081	-0.413	-4.281
0.3019	-1.021	-0.205	-0.316	0.305	0.077	-0.600	-5.577
0.3937	-1.078	-0.197	-0.324	0.297	0.054	-0.500	-6.366
0.5023	-1.044	-0.170	-0.302	0.259	0.008	-0.662	-6.718
0.5840	-0.960	-0.142	-0.267	0.218	-0.030	-0.403	-6.558
0.6946	-0.780	-0.100	-0.203	0.154	-0.075	-0.557	-5.756
0.7788	-0.602	-0.068	-0.147	0.104	-0.092	-0.460	-4.689
0.8707	-0.373	-0.036	-0.083	0.054	-0.084	-0.178	-3.074
318.15 K							
0.1011	-0.541	-0.137	-0.181	0.188	0.049	-0.101	-2.404
0.2059	-0.886	-0.201	-0.289	0.284	0.073	-0.403	-4.396
0.3019	-1.056	-0.217	-0.336	0.313	0.070	-0.587	-5.733
0.3937	-1.114	-0.209	-0.346	0.306	0.047	-0.487	-6.551
0.5023	-1.078	-0.180	-0.322	0.267	0.004	-0.647	-6.920
0.5840	-0.990	-0.151	-0.285	0.225	-0.033	-0.390	-6.760

Table 3 (continued)

x_1	V_m^E 10 ⁶ /m ³ mol ⁻¹	κ_s^E 10 ¹⁰ /m ² N ⁻¹	$K_{s,m}^E$ 10 ¹⁴ /m ⁵ N ⁻¹ mol ⁻¹	u^E 10 ⁻² /m s ⁻¹	10 ⁶ · ΔR_M /m ³ mol ⁻¹	10 ² · $\Delta_\phi n_D$	α_p^E /kK ⁻¹
0.6946	- 0.805	- 0.107	- 0.217	0.160	- 0.076	- 0.545	- 5.937
0.7788	- 0.621	- 0.073	- 0.157	0.109	- 0.092	- 0.450	- 4.840
0.8707	- 0.384	- 0.039	- 0.089	0.057	- 0.083	- 0.173	- 3.174
323.15 K							
0.1011	- 0.564	- 0.146	- 0.193	0.191	0.043	- 0.098	- 2.477
0.2059	- 0.923	- 0.214	- 0.308	0.290	0.064	- 0.395	- 4.538
0.3019	- 1.099	- 0.231	- 0.358	0.321	0.059	- 0.576	- 5.926
0.3937	- 1.158	- 0.222	- 0.369	0.314	0.037	- 0.476	- 6.779
0.5023	- 1.121	- 0.192	- 0.343	0.275	- 0.004	- 0.635	- 7.168
0.5840	- 1.028	- 0.161	- 0.304	0.232	- 0.039	- 0.380	- 7.007
0.6946	- 0.835	- 0.114	- 0.232	0.165	- 0.079	- 0.534	- 6.159
0.7788	- 0.644	- 0.078	- 0.168	0.113	- 0.094	- 0.441	- 5.023
0.8707	- 0.398	- 0.041	- 0.095	0.059	- 0.084	- 0.168	- 3.295

Standard uncertainty $s(T) = \pm 0.01$ K, $s(x) = \pm 1.0 \times 10^{-4}$, $s(\rho) = \pm 0.8$ kg m⁻³, $s(u) = \pm 1$ m s⁻¹, $s(n_D) = \pm 0.0005$, $s(T)$ for n_D = ± 0.02 K, $s(p) = \pm 1.0$ kPa

The deviation of V_m^E , κ_s^E , $K_{s,m}^E$, u^E and ΔR_m with mole fraction of [Bmim][PF₆] and temperature for the studied binary mixtures along with smoothed R–K equation values (Table 4) are graphically depicted in Figs. 2, 4–7 at T /K = 298.15–323.15, respectively.

It has been stated [37–40] that V_m^E and κ_s^E values of the binary mixtures result from the contributions due to the physical, chemical and structural characteristics of the component liquids. The physical contributions comprise dispersion forces and non-specific physical (weak) interactions, which lead to positive V_m^E and κ_s^E values. The chemical contributions involve breaking up the associates present in the pure liquids, resulting in positive V_m^E and values. These contributions also involve specific interactions such as formation of H-bonding, charge transfer (donor–acceptor) complexes, and ion–dipole interactions between the component molecules of the mixture, resulting in negative V_m^E and κ_s^E values. The structural contributions are due to the geometrical fitting (favourable/unfavourable) of the molecules of very different molecular sizes into each other's structures resulting in negative or positive V_m^E and κ_s^E values.

Instead of our craving, the negative V_m^E values suggest the formation of strong ion–dipole interactions between ions formed by ionic liquid [Bmim⁺] and [PF₆⁻] and dipoles of NVP molecules. In this present binary system, the structural contributions are predominant. The composition and temperature dependence of V_m^E for the studied mixtures may be explained based on structural contributions arising from interstitial accommodation and changes of free volume. Another source of negative contribution to V_m^E may be from the fitting of small NVP molecules (molar

volume: NVP = 106.93 cm³ mol⁻¹ at T = 298.15 K) into the voids present in bigger [Bmim][PF₆] molecules (molar volumes = 207.85 cm³ mol⁻¹ at T = 298.15 K). Contributions emerging from the geometrical fitting of smaller molecules into the voids accessible in the structure of bigger molecules were likewise considered by others [40, 41] for translating negative V_m^E values for binary mixtures that contains molecules of different molecular sizes. Therefore, the geometrical impact due to interstitial fitting of NVP molecules in the interstices of ionic liquids, and the ion–dipole interactions between highly polar NVP molecules and imidazolium ring of the ionic liquids contributes to the negative values of V_m^E [42, 43].

There is a systematic decrease in V_m^E for all the systems with the rise in temperature. A comparison of the data at different temperatures reveals that the temperature coefficient

$$\left(\frac{\partial V_m^E}{\partial T}\right)_p$$

is negative, indicating that there is a formation of associated species between [Bmim][PF₆] + NVP mixture with a rise in temperature, which results in a contraction in volume of the mixture and hence negative V_m^E values.

We graphically compared our V_m^E results with the mixtures of 1-butyl-3-methylimidazolium with different anions BF₄ [9], PF₆ and NTf₂ [10] in Fig. 3 at 298.15 K. The degree of their influence depends on the nature of anion and cation of the ionic liquids, and the nature of the organic compounds. This suggests that the strength of interactions in these mixtures follows the sequence of [Bmim][PF₆] > [Bmim][BF₄] > [Bmim][NTf₂].

Table 4 Coefficients A_i of Eq. (10) along with standard deviations σ of binary mixture properties

T/K	A_1	A_2	σ	SE	F -value	p value
V_m^E 10^6 m^3 mol^{-1}						
298.15	- 3.787	1.302	0.353	0.013	13,772.50	7.11×10^{-15}
303.15	- 3.935	1.367	0.367	0.014	13,769.49	7.11×10^{-15}
308.15	- 4.088	1.433	0.381	0.015	13,980.95	6.69×10^{-15}
313.15	- 4.250	1.502	0.396	0.015	13,410.77	7.91×10^{-15}
318.15	- 4.391	1.569	0.410	0.016	12,642.82	1.00×10^{-14}
323.15	- 4.563	1.649	0.426	0.017	12,349.60	1.10×10^{-14}
κ_s^E 10^{10} m^2 N^{-1}						
298.15	- 0.591	0.563	0.064	0.008	1182.19	1.29×10^{-10}
303.15	- 0.635	0.592	0.068	0.008	1219.77	1.14×10^{-10}
308.15	- 0.677	0.624	0.073	0.008	1251.73	1.03×10^{-10}
313.15	- 0.718	0.657	0.077	0.009	1256.32	1.01×10^{-10}
318.15	- 0.764	0.694	0.082	0.009	1265.00	9.87×10^{-11}
323.15	- 0.812	0.735	0.087	0.010	1266.58	9.82×10^{-11}
$K_{s,m}^E$ 10^{14} m^5 N^{-1} mol^{-1}						
298.15	- 0.998	0.603	0.099	0.003	20,593.72	1.42×10^{-15}
303.15	- 1.076	0.630	0.106	0.003	20,283.25	1.51×10^{-15}
308.15	- 1.151	0.665	0.113	0.003	20,446.22	1.46×10^{-15}
313.15	- 1.225	0.702	0.120	0.004	19,676.84	1.71×10^{-15}
318.15	- 1.307	0.743	0.128	0.004	19,239.39	1.87×10^{-15}
323.15	- 1.394	0.791	0.137	0.004	18,695.73	2.09×10^{-15}
μ^E 10^2 m s^{-1}						
298.15	0.979	- 0.924	0.107	0.010	1814.67	2.34×10^{-11}
303.15	1.020	- 0.928	0.110	0.010	2016.31	1.54×10^{-11}
308.15	1.054	- 0.936	0.113	0.010	2201.12	1.08×10^{-11}
313.15	1.080	- 0.942	0.115	0.010	2388.76	7.81×10^{-12}
318.15	1.113	- 0.953	0.118	0.009	2601.76	5.55×10^{-12}
323.15	1.144	- 0.967	0.121	0.009	2812.94	4.07×10^{-12}
ΔR_m 10^6 m^3 mol^{-1}						
298.15	0.076	- 1.027	0.072	0.006	636.98	1.52×10^{-09}
303.15	0.041	- 0.991	0.070	0.007	553.63	2.65×10^{-09}
308.15	0.019	- 0.951	0.067	0.007	475.89	4.83×10^{-09}
313.15	0.007	- 0.905	0.064	0.007	401.49	9.47×10^{-09}
318.15	- 0.012	- 0.866	0.061	0.007	339.15	1.85×10^{-09}
323.15	- 0.046	- 0.825	0.058	0.008	293.19	3.28×10^{-09}
n_D^E 10^2						
298.15	- 24.141	- 0.527	2.224	0.010	636.98	1.52×10^{-09}
303.15	- 24.999	- 0.652	2.304	0.012	553.63	2.65×10^{-09}
308.15	- 25.881	- 0.765	2.386	0.013	475.89	4.83×10^{-09}
313.15	- 26.803	- 0.888	2.471	0.015	401.49	9.47×10^{-09}
318.15	- 27.603	- 1.036	2.546	0.017	339.15	1.85×10^{-08}
323.15	- 28.585	- 1.203	2.638	0.019	293.19	3.28×10^{-08}

An ultrasonic study is one of the best tools to understand the nature of interactions between solute–solute and solute–solvent or solvent–solvent in the mixture [44]. Nonlinear variation of κ_s^E and $K_{s,m}^E$ as a function of [Bmim][PF₆] of the liquid mixture is sufficient evidence for the existence of molecular interactions in solutions. A

perusal of Figs. 4 and 5 also shows that κ_s^E and $K_{s,m}^E$ values become more negative as the temperature is increased from 298.15 to 323.15 K. With the increase in temperature, the kinetic energy of the molecules increases, and a large number of free NVP molecules would be available in the mixture due to breaking of hydrogen bonds and move

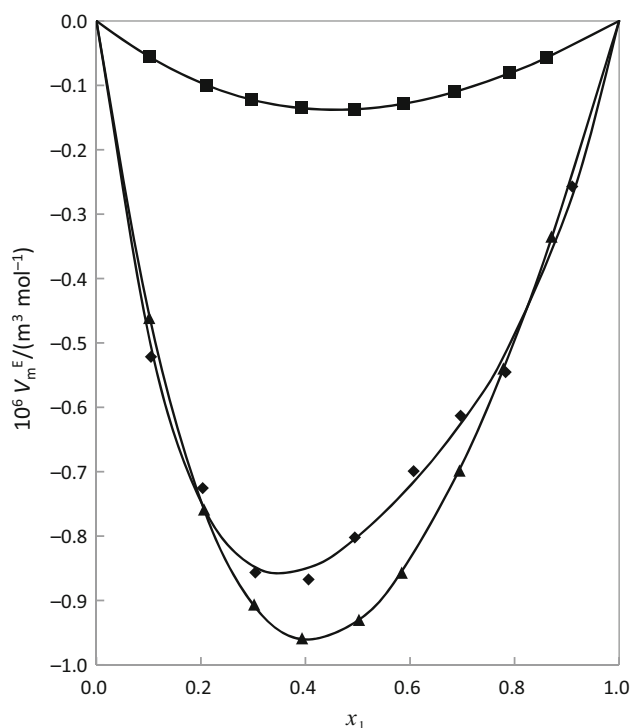


Fig. 3 Comparative excess molar volume of NVP for [BMIM][NTf2] (■); [BMIM][BF₄] (◆); [BMIM][PF₆] (▲) at $T/K = 298.15$

towards C₂ atom of imidazolium ring due to completely dissociated ionic liquid at higher temperature. Therefore, at higher temperature the ion–dipole interactions between unlike molecules (ions from ionic liquid and dipoles of NVP) become more significant due to availability of greater number of amide dipoles, leading to the contraction in volume, thereby decreasing the volume and compressibility of the mixture. This may be explained as follows:

The one kind of properties of imidazolium cations is established in the electrostatic attraction of the aromatic cations. The electrostatic fascination of these salts contains delocalized 3-centre-4-electron configuration across the N₁–C₂–N₃ moiety, a twofold bond between C₄ and C₅ at the inverse side of the ring and a powerless delocalization in the central region [45]. The hydrogen radicals C₂–H, C₄–H, and C₅–H convey nearly a similar charge, yet carbon C₂ is decidedly charged inferable from the electron deficiency in the C=N bond, whereas C₄ and C₅ are practically neutral. The subsequent causticity of the hydrogen atoms is the key tip to comprehend the properties of these ionic liquids. The hydrogen on the C₂ carbon (C₂–H) has been appeared to cling particularly with the solute molecules [46, 47]. It appears to be that the hydrogen atom at C₂ (between nitrogen atoms) can be viewed as acidic to shape a strong hydrogen bond with oxygen atom of NVP. This presumption has been affirmed by Crosthwaite et al. [48].

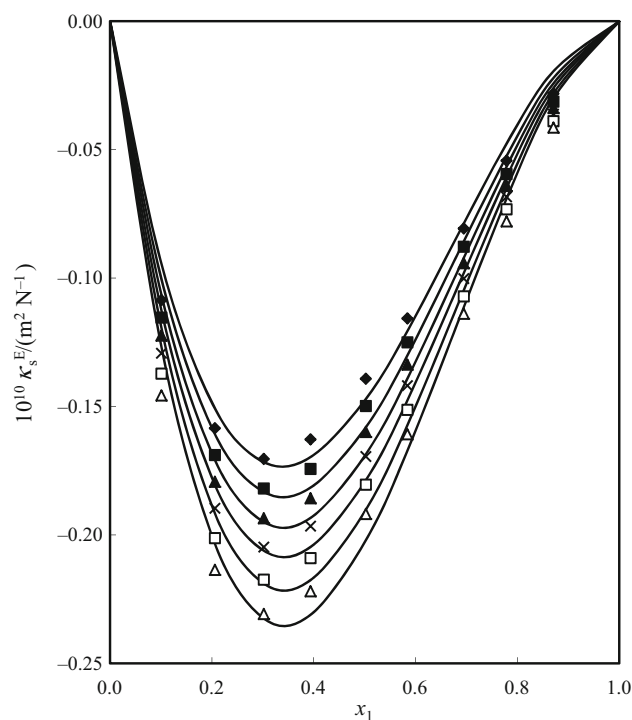


Fig. 4 Plots of excess molar compressibility, κ_s^E versus mole fraction, x_1 of [Bmim][PF₆] for [Bmim][PF₆] + NVP binary mixtures at temperatures, $T/K = 298.15$, ◆; At $T/K = 303.15$, ■; $T/K = 308.15$, ▲; $T/K = 313.15$, ×; $T/K = 318.15$, □; $T/K = 323.15$, △. The points represent experimental values, and lines represent values calculated from Eq. (10) using the coefficients given in Table 4

As expected, the u^E exhibit positive values in the binary mixture at the investigated temperature range. In general, positive deviations in u^E indicate the presence of significant interactions and negative deviations in u^E indicate weak interactions between the unlike molecules in the mixtures [49, 50]. The positive u^E values suggest the formation of significant ion–dipole interactions between the ions [Bmim⁺] and [PF₆[−]] formed by ionic liquid and dipoles of NVP molecules. At higher mole fractions ($x_1 > 0.9$), the interactions between like molecules IL–IL and NVP–NVP seem dominating in these binary mixtures. The observed positive values of u^E for these binary mixtures indicate strong interactions involving the formation of ion–dipole and hydrogen bonding between the component molecules of the mixture. Thus, the trends of u^E versus x_1 (Fig. 6) strongly support the behaviour of V_m^E and κ_s^E for these mixtures.

The results presented in Fig. 5S indicate that $\Delta_\phi n_D$ values are negative for these mixtures over the entire mole fraction range at all investigated temperatures. In general, the positive deviations in Δn values (on volume fraction dependence basis) are considered due to the presence of

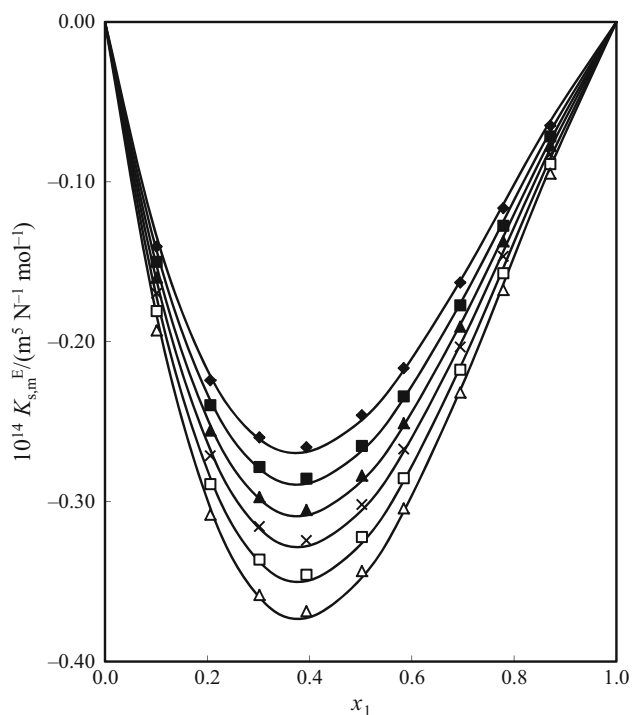


Fig. 5 Excess molar isentropic compressibilities $K_{s,m}^E$ versus mole fraction, x_1 of [Bmim][PF₆] for [Bmim][PF₆] + NVP binary mixtures at temperatures, $T/K = 298.15$, \blacklozenge ; At $T/K = 303.15$, \blacksquare ; $T/K = 308.15$, \blacktriangle ; $T/K = 313.15$, \times ; $T/K = 318.15$, \square ; $T/K = 323.15$, \triangle . The points represent experimental values, and lines represent values calculated from Eq. (10) using the coefficients given in Table 4

significant interactions in the mixtures, whereas negative deviations in $\Delta_\phi n_D$ values indicate weak interactions between the components of the mixture [51]. The $\Delta_\phi n_D$ values decrease with the increase in temperature for each binary mixture, indicating that the ion–dipole interactions between unlike molecules decrease due to less availability of NVP dipoles.

The outcomes introduced in Fig. 7 demonstrate that ΔR_m values likewise show sigmoid pattern with positive ΔR_m values at low mole parts ($x_1 < 0.5$) of [Bmim][PF₆] and negative ΔR_m values at higher mole parts ($x_1 > 0.5$) of [Bmim][PF₆] in these binary mixtures at each examined temperature. Positive values of ΔR_m indicate strong intermolecular interactions, while negative values indicate weak intermolecular interactions (dispersion forces/ion–dipole interactions). All in all, the positive deviations in ΔR_m values (on volume part reliance premise) are considered because of nearness of huge communications in the mixtures, though negative deviations in ΔR_m values indicate frail collaborations between the segments of the mixture [30, 51]. The ΔR_m values increase with the increase in temperature for this binary mixture,

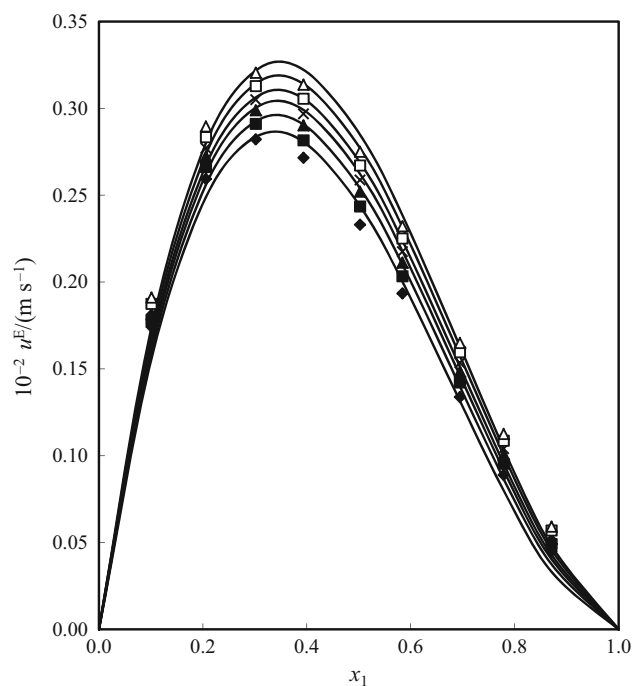


Fig. 6 Excess speed of sound u^E versus mole fraction, x_1 of [Bmim][PF₆] for [Bmim][PF₆] + NVP binary mixtures at temperatures, $T/K = 298.15$, \blacklozenge ; At $T/K = 303.15$, \blacksquare ; $T/K = 308.15$, \blacktriangle ; $T/K = 313.15$, \times ; $T/K = 318.15$, \square ; $T/K = 323.15$, \triangle . The points represent experimental values, and lines represent values calculated from Eq. (10) using the coefficients given in Table 4

demonstrating that the ion–dipole interactions between dissimilar molecules increase because of accessibility of more NVP dipoles on softening of affiliations present in ideal NVP.

A comparison of isobaric thermal expansivity (α_p) data in Table 2S with reported values reveals a fairly consistent between the two, and the AAD between both was $\pm 0.4\%$ for IL and NVP is $\pm 0.1\%$ which can be considered quite acceptable. Thus, the density data were precise enough to allow the accurate determination of the temperature dependence of α_p for liquids using the incremental method. Here in our case the density values are linearly decrement w.r.t temperature. Figure 6S shows the α_p^E values obtained against composition; it is clearly observed that mixtures exhibit relatively small or negligible change in this excess quantity.

Partial molar quantities

A perusal of Figs. 8 and 9 (Supplementary material Tables 3S & 4S) indicates that the values of $\bar{V}_{m,1}^E$ and $\bar{V}_{m,2}^E$; $\bar{K}_{s,m,1}^E$ and $\bar{K}_{s,m,2}^E$ are negative for both the binary mixtures over the whole composition range. This suggests that the molar volumes (or) molar isentropic compressibilities of

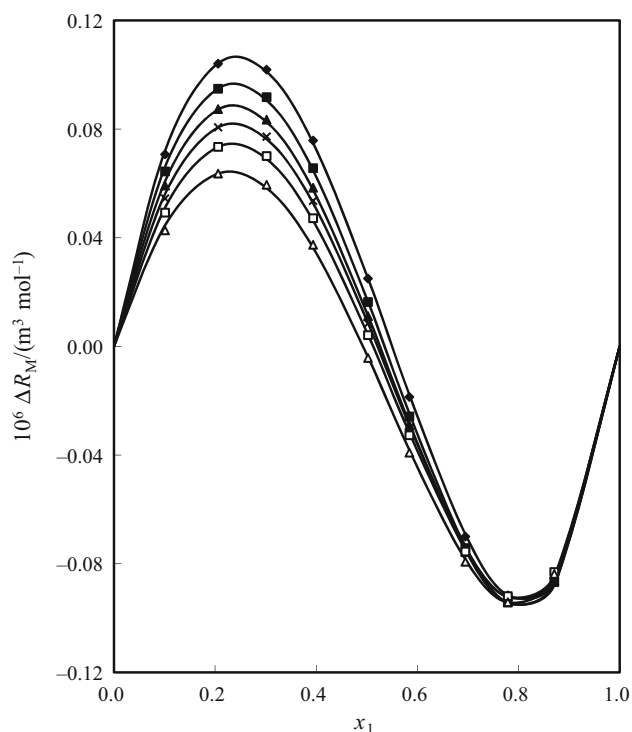


Fig. 7 Deviation in molar refraction ΔR_M versus mole fraction, x_1 of [Bmim][NTf₂] for [Bmim][NTf₂] + NVP binary mixtures at temperatures, $T/K = 298.15$, \blacklozenge ; At $T/K = 303.15$, \blacksquare ; $T/K = 308.15$, \blacktriangle ; $T/K = 313.15$, \times ; $T/K = 318.15$, \square ; $T/K = 323.15$, \triangle . The points represent experimental values, and lines represent values calculated from Eq. (10) using the coefficients given in Table 4

each component in the mixture are less than their respective molar volume (or) molar isentropic compressibilities in the pure state, *i.e.* there is a decrease in the volume (or) isentropic compressibilities on mixing [Bmim][PF₆] with NVP. In general, the negative $\bar{V}_{m,1}^E$ and $\bar{V}_{m,2}^E$; $\bar{K}_{s,m,1}^E$ and $\bar{K}_{s,m,2}^E$ values indicate the presence of significant solute-solvent interactions between unlike molecules, whereas the positive $\bar{V}_{m,1}^E$ and $\bar{V}_{m,2}^E$; $\bar{K}_{s,m,1}^E$ and $\bar{K}_{s,m,2}^E$ values indicate the presence of weak interactions [52] in the mixture. The observed negative $\bar{V}_{m,1}^E$ and $\bar{V}_{m,2}^E$; $\bar{K}_{s,m,1}^E$ and $\bar{K}_{s,m,2}^E$ values indicate that [Bmim][PF₆] – NVP interactions are stronger than interactions between like molecules which lead to decrease in volume and compressibility.

A look at Tables 5 and 6 indicates that the values of $\bar{V}_{m,1}^{\circ E}$ and $\bar{V}_{m,2}^{\circ E}$; $\bar{K}_{s,m,1}^{\circ E}$ and $\bar{K}_{s,m,2}^{\circ E}$ are negative for these binary systems at each investigated temperature. This suggests that the V_m or $K_{s,m}$ of each component in the mixture is less than their respective V_m or $K_{s,m}$ in the pure state, *i.e.* there is a contraction in volume or decrease in the $K_{s,m}$ on mixing [Bmim][PF₆] with NVP. The observed negative $\bar{V}_{m,1}^{\circ E}$ and $\bar{V}_{m,2}^{\circ E}$ values indicate that [Bmim][PF₆]-

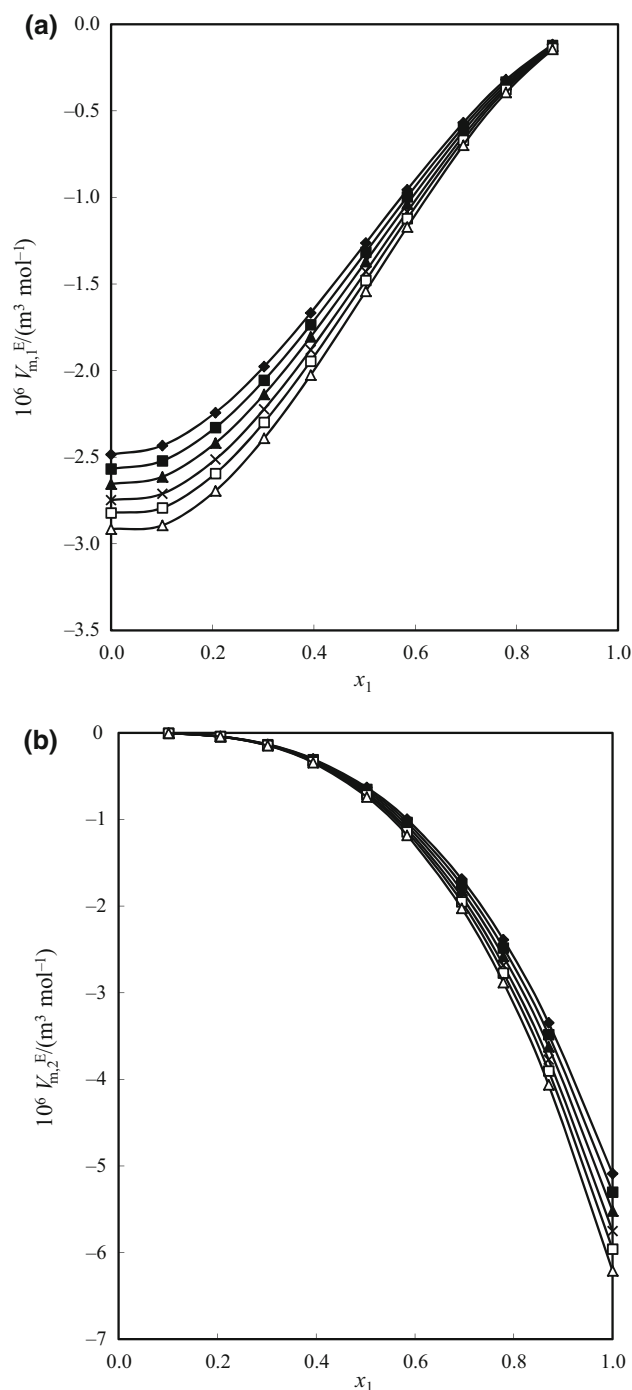


Fig. 8 Variation of excess partial molar volumes, $\bar{V}_{m,1}^E$ and $\bar{V}_{m,2}^E$ of **a** [Bmim][PF₆] and **b** NVP, respectively, of against mole fraction, x_1 of [Bmim][PF₆] for the binary mixtures at temperatures, $T/K = 298.15$, \blacklozenge ; At $T/K = 303.15$, \blacksquare ; $T/K = 308.15$, \blacktriangle ; $T/K = 313.15$, \times ; $T/K = 318.15$, \square ; $T/K = 323.15$, \triangle

NVP interactions are stronger than interactions between like molecules.

The values of $\bar{V}_{m,1}^{\circ E}$ and $\bar{V}_{m,2}^{\circ E}$; $\bar{K}_{s,m,1}^{\circ E}$ and $\bar{K}_{s,m,2}^{\circ E}$ can be analysed in terms of structural and geometrical compressibility as suggested by Hall and others [52–54]. The

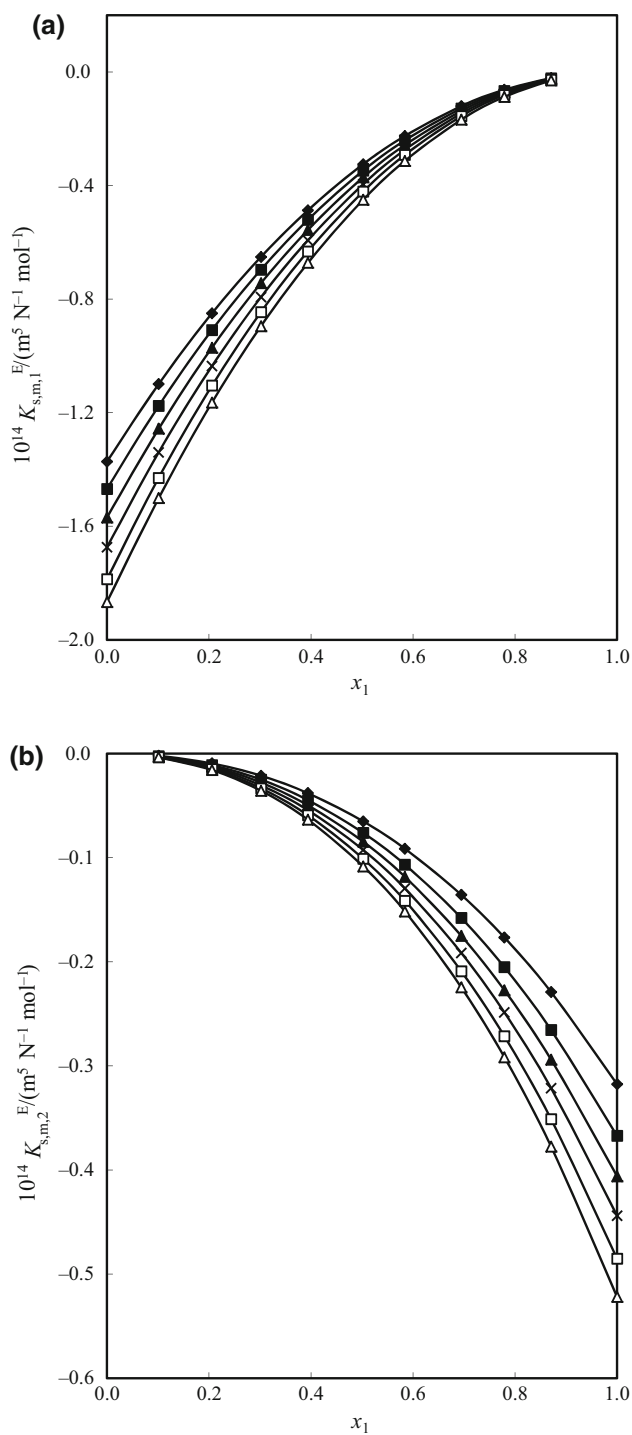


Fig. 9 Variation of excess partial molar isentropic compressibilities, $\bar{K}_{s,m,1}^E$ and $\bar{K}_{s,m,2}^E$ of (a) [Bmim][NTf₂] and (b) NVP, respectively, of against mole fraction, x_1 of [Bmim][NTf₂] for the binary mixtures at temperatures, $T/K = 298.15$, \blacklozenge ; At $T/K = 303.15$, \blacksquare ; $T/K = 308.15$, \blacktriangle ; $T/K = 313.15$, \times ; $T/K = 318.15$, \square ; $T/K = 323.15$, \triangle

structural compressibility results from the breakdown of associated structure (on mixing [Bmim][PF₆] with NVP), whereas geometrical compressibility is due to the

simultaneous compression of the molecules (due to specific interactions between [Bmim][PF₆] and NVP molecules) leading to contraction in volume and decrease in compressibility. The observed values of $\bar{V}_{m,1}^{\circ E}$ and $\bar{V}_{m,2}^{\circ E}$; $\bar{K}_{s,m,1}^{\circ E}$ and $\bar{K}_{s,m,2}^{\circ E}$ indicate that the geometrical compressibility factor dominates in these mixtures. Also, $\bar{V}_{m,1}^{\circ E}$ and $\bar{V}_{m,2}^{\circ E}$; $\bar{K}_{s,m,1}^{\circ E}$ and $\bar{K}_{s,m,2}^{\circ E}$ values decrease with the increase in temperature (Tables 5 and 6) for each binary mixture which further supports the trends observed in V_m^E and κ_s^E values.

Prediction of refractive index using mixing rules

Refractive index of liquid mixtures is an important property for structural characterization, engineering calculations and assessing purity of substance. The refractive index is used in the continuum model of matter and parameterizes how matter interacts with electromagnetic polarizability (Kier and Hall) to estimate the boiling point with Meissner's method or to estimate the other thermodynamic properties. Measurement of refractive index can be used for providing information about the forces between the molecules [55] or their behaviour when they are in solution [56]. The refractive indices of the binary mixtures have been theoretically calculated from the refractive index data of pure components of the mixtures using nine mixing rules [39]. There exist the definite expansion and/or contraction of liquid when the mixing takes place and also densities become changed, and due to this density change, we observe a considerable variation in refractive index. This was firstly examined by Laplace and later by Gladstone–Dale who gave a formula for the determination of refractive index of a liquid mixture by using the properties of their pure components and has been used for optical analysis (determination of composition), or to calculate the density of a liquid for use in fluid dynamics such as flow visualization. We have various empirical and semi-empirical relations that have been formulated in this connection, and it is found out that rules due to Lorentz–Lorentz and Weiner are extensively used. It is important to mention that there exists a drawback of these mixing rules in their inability to account for changes in volume and refractivity during mixing; this is because of volume additivity. In the light of above description, it is fully feasible to make discussion for these mixing rules for the mixtures taken in this study. The values are seen to decrease with the increase in temperature for pure components as well as mixtures, but the AAPD values tend to increase with temperature which can be accounted by the changing density and nonlinear

Table 5 Values $\bar{V}_{m,1}^{\circ}$, $\bar{V}_{m,1}^{*}$, $\bar{V}_{m,1}^{\circ E}$, $\bar{V}_{m,2}^{\circ}$, $\bar{V}_{m,2}^{*}$, $\bar{V}_{m,2}^{\circ E}$ of the components for [Bmim] [PF₆] + NVP at temperatures $T = 298.15$ – 323.15 K

T/K	$10^6 \bar{V}_{m,1}^{\circ} \text{ m}^3 \text{ mol}^{-1}$	$10^6 \bar{V}_{m,1}^{*}$	$10^6 \bar{V}_{m,1}^{\circ E}$	$10^6 \bar{V}_{m,2}^{\circ}$	$10^6 \bar{V}_{m,2}^{*}$	$10^6 \bar{V}_{m,2}^{\circ E}$
298.15	304.24	306.73	– 2.48	101.84	106.93	– 5.09
303.15	305.12	307.69	– 2.57	102.08	107.39	– 5.30
308.15	305.99	308.65	– 2.66	102.32	107.85	– 5.52
313.15	306.87	309.62	– 2.75	102.56	108.31	– 5.75
318.15	307.77	310.60	– 2.82	102.82	108.78	– 5.96
323.15	308.66	311.58	– 2.91	103.04	109.25	– 6.21

Table 6 Values $\bar{K}_{s,m,1}^{\circ}$, $K_{s,m,1}^{*}$, $\bar{K}_{s,m,1}^{\circ E}$, $\bar{K}_{s,m,2}^{\circ}$, $K_{s,m,2}^{*}$ and $\bar{K}_{s,m,2}^{\circ E}$ of the components for [Bmim] [PF₆] + NVP at temperatures $T = 298.15$ – 323.15 K

T/K	$10^{14} \bar{K}_{s,m,1}^{\circ}$ ($\text{m}^5 \text{ N}^{-1} \text{ mol}^{-1}$)	$10^{14} K_{s,m,1}^{*}$	$10^{14} \bar{K}_{s,m,1}^{\circ E}$	$10^{14} \bar{K}_{s,m,2}^{\circ}$	$10^{14} K_{s,m,2}^{*}$	$10^{14} \bar{K}_{s,m,2}^{\circ E}$
298.15	5.917	7.289	– 1.373	4.122	4.439	– 0.318
303.15	5.990	7.458	– 1.468	4.223	4.590	– 0.367
308.15	6.062	7.631	– 1.569	4.340	4.747	– 0.406
313.15	6.131	7.805	– 1.674	4.466	4.910	– 0.444
318.15	6.196	7.983	– 1.787	4.594	5.079	– 0.485
323.15	6.296	8.163	– 1.867	4.734	5.256	– 0.522

Table 7 Average percentage deviations (APDs) in theoretically calculated refractive indices by using Arago–Biot (A–B), Gladstone–Dale (G–D), Newton (N), Eyring and John (E–J), Lorentz–Lorentz (L–L), Heller (H), Eykman (EK), Oster (OS), and Weiner (W) relations for [Bmim][PF₆] + NVP binary mixtures at temperatures $T/K = 298.15$ – 323.15

T/K	Average percentage deviations (APDs)								
	A–B	G–D	N	E–J	L–L	H	EK	OS	W
298.15	0.151	0.151	0.117	0.170	0.192	0.184	0.247	0.274	0.166
303.15	0.151	0.151	0.117	0.170	0.192	0.183	0.246	0.272	0.166
308.15	0.153	0.153	0.118	0.172	0.193	0.184	0.247	0.273	0.168
313.15	0.156	0.156	0.121	0.175	0.197	0.187	0.249	0.275	0.171
318.15	0.158	0.158	0.123	0.176	0.198	0.188	0.250	0.275	0.172
323.15	0.158	0.158	0.123	0.177	0.198	0.189	0.250	0.274	0.173

behaviour between molecules as reflected by refractive index evaluation [57]. Among all equations proposed to estimate the refractive index of the mixtures from the pure components, Newton relation was found best other than equations. APD of the mixture at all studied temperatures is summarized in Table 7 and follows the sequence Oster > Eykman > Lorentz–Lorenz > Heller > Eyring and John > Weiner > Arago–Biot \geq Gladstone–Dale > Newton.

FTIR analysis

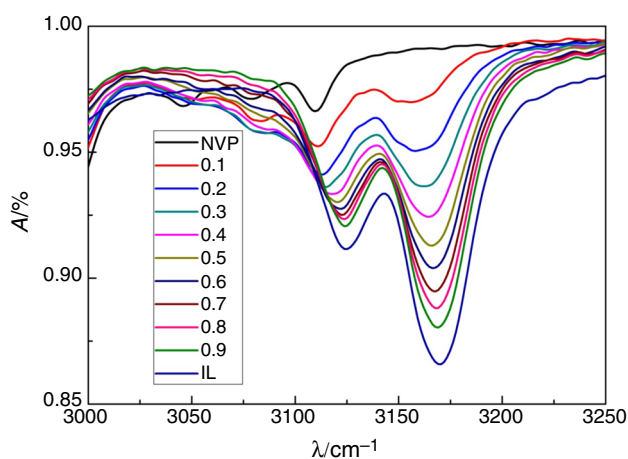
The nature and degree of collaborations between the ILs and natural solvents are all around reported through thermodynamic reviews and are not adequate to determine the correct way of solute-dissolvable communications between

the connecting segments. To accomplish this objective, here we analysed the intermolecular interactions between the ionic liquid [Bmim][PF₆] and NVP at atomic level over the entire creation extend utilizing FTIR spectroscopy. It is an important tool for recognizable of little change in dipole moments.

The infrared spectra for pure [Bmim][PF₆], NVP and their binary mixtures are shown in Fig. 7S (*Supplementary material*) and are summarized in Table 8. In 1-butyl-3-methylimidazolium cation, the CH stretching region between 2800 and 3200 cm^{-1} was analysed. For [Bmim][PF₆], the signals in this region can be split into two parts: (1) the signals between 2800 and 3000 cm^{-1} result from aliphatic CH groups in the butyl and methyl moieties, (2) signals between 3000 and 3200 cm^{-1} can be assigned to CH modes predominantly originating from the aromatic imidazolium ring, from C₂–H and C_{4,5}–H stretching

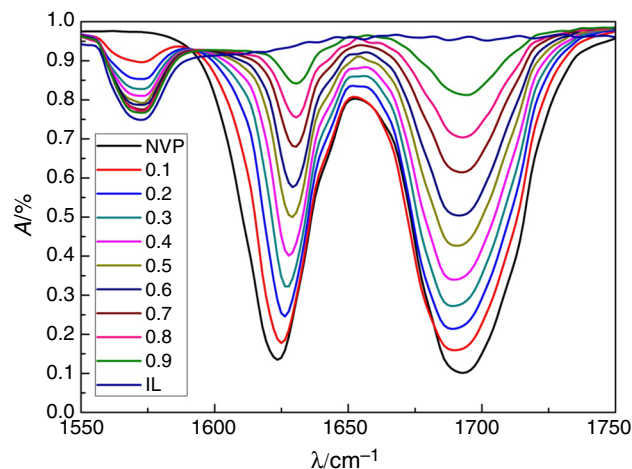
Table 8 Infrared transmittance wave numbers between [Bmim][PF₆] in NVP at room temperature and atmospheric pressure $P = 0.1$ MPa

IL	NVP	C–H	C ₂ –H	C _{4,5} – H	C=O	C=N	P–F
0.0000	1.0000	–	3109.6	–	1692.9	–	–
0.1011	0.8989	2961.6	3111.0	3156.3	1690.1	623.3	745.1
0.2059	0.7941	2962.3	3112.4	3157.8	1688.7	623.3	748.0
0.3019	0.6981	2962.3	3115.3	3162.0	1688.7	623.3	748.0
0.3937	0.6063	2963.7	3118.1	3164.8	1690.1	621.9	748.7
0.5023	0.4977	2963.7	3120.9	3166.3	1690.1	621.9	748.7
0.5840	0.4160	2963.7	3122.3	3166.3	1691.5	621.9	748.7
0.6946	0.3054	2965.1	3123.8	3167.7	1692.9	621.9	748.7
0.7788	0.2212	2965.1	3124.2	3169.1	1692.9	621.9	748.7
0.8707	0.1293	2965.1	3124.8	3170.5	1692.9	621.9	749.4
1.0000	0.0000	2966.5	3126.6	3170.5	–	621.9	749.4


Fig. 10 IR spectra for [Bmim][PF₆] + NVP mixtures in the range of 3000–3250 cm^{-1}

frequencies. The C₂–H vibrational frequency (3124.7 cm^{-1}) is shifted by about 44.8 cm^{-1} to lower frequencies than the C₄–H and C₅–H stretches (3169.5 cm^{-1}) due to its stronger acidic character. The pure liquid NVP has two very strong vibration bands in the IR spectrum at 1629 and 1692.9 cm^{-1} corresponding to C=C and C=O stretching frequencies, respectively. There is a possibility for conjugation of olefinic group with the carbonyl group through electron pair of the nitrogen. Due to the resonance system involving five atoms, C=C and C=O stretching frequencies are inter dependable.

In the present mixture, observable changes were noticed between the frequencies of 3000–3200 cm^{-1} which belong to C₂–H and C_{4,5}–H stretching frequencies of imidazolium cation as well as C=O and C=C stretching frequencies of NVP. As mole fraction of NVP increases, a blue shift in C₂–H and C_{4,5}–H stretching frequencies indicates the


Fig. 11 IR spectra for [Bmim][PF₆] + NVP mixtures in the range of 1550–1750 cm^{-1}

formation of hydrogen bond between [Bmim]⁺ and NVP as C₂–H and C_{4,5}–H experience weak hydrogen bonding interactions than in pure [Bmim][PF₆]. The blue shift is very predominant in C₂–H frequencies when compared to C_{4,5}–H stretching frequencies which indicates that more acidic C₂–H plays a major role in the formation of hydrogen bond with carbonyl oxygen of NVP (Fig. 10). Simultaneously, as mole fraction of IL increases a clear red shift in C=O and C=C Sym stretch frequencies are observed in NVP. This clearly indicates the formation of intermolecular hydrogen bond between hydrogen of aromatic imidazolium ring and carbonyl oxygen of NVP (Fig. 11). Ion–dipole interactions can also explain on the basis of anion [PF₆][−] with NVP. A blue shift was observed in P–F of [PF₆][−] anion by the addition of NVP.

Conclusions

The present study reported the densities, ρ , speeds of sound, u and refractive indices, n_D of the binary mixtures of [Bmim][PF₆] with NVP over whole composition range at different temperatures. From the experimental data, various physicochemical parameters, viz. V_m^E , κ_s^E , u^E , $K_{s,m}^E$ and $\Delta_\phi n_D$ of the mixtures; $\bar{V}_{m,1}$ and $\bar{V}_{m,2}$, $\bar{K}_{s,m,1}$ and $\bar{K}_{s,m,2}$, $\bar{V}_{m,1}^E$ and $\bar{V}_{m,2}^E$ and $\bar{K}_{s,m,1}^E$ and $\bar{K}_{s,m,2}^E$ over whole composition range; $\bar{V}_{m,1}^\circ$ and $\bar{V}_{m,2}^\circ$; $\bar{K}_{s,m,1}^\circ$ and $\bar{K}_{s,m,2}^\circ$; $\bar{V}_{m,1}^{\circ E}$ and $\bar{V}_{m,2}^{\circ E}$ and $\bar{K}_{s,m,1}^{\circ E}$ and $\bar{K}_{s,m,2}^{\circ E}$ of the components infinite dilution have been calculated. The results have been discussed in terms of intermolecular interactions in these mixtures. The results indicate the formation of strong ion–dipole interactions between ionic liquid [Bmim][PF₆] and NVP molecules and the geometrical effect due to interstitial fitting of smaller NVP molecules into the interstices of ionic liquid

molecules. The FTIR spectra of these mixtures have also been recorded at 298.15 K and analysed in terms of intermolecular interactions. FTIR spectra results further supported the above conclusions regarding interactions in these mixtures. The V_m^E values for these mixtures are predicted well by PFP theory. The refractive index data are well correlated by various mixing rules. All the equations used for predicting refractive index exhibit excellent agreement and generate AAPD values much below 1%. The strength of interactions of 1-butyl-3-methylimidazolium with different anions follows the sequence of [Bmim][PF₆] > [Bmim][BF₄] > [Bmim][NTf₂].

Acknowledgements P. Suneetha was thankful to the CSIR, India, for the award of Senior Research Fellowship. The authors were also thankful to Arvind kumar, Principal Scientist, CSMCRI, India, for providing the research facilities.

Compliance with ethical standards

Conflict of interest The authors declare no competing financial interest.

References

- Iloukhani H, Samiey B, Moghaddasi MA. Speeds of sound, isentropic compressibilities, viscosities and excess molar volumes of binary mixtures of methylcyclohexane + 2-alkanols or ethanol at T = 298.15 K. *J Chem Thermodyn.* 2006;38:190–200.
- Tome LI, Carvalho PJ, Freire MG, Marrucho IM, Fonseca IM, Ferreira AG, Coutinho JA, Gardas RL. Measurements and correlation of high-pressure densities of imidazolium-based ionic liquids. *J Chem Eng Data.* 2008;53:1914–21.
- Korokin A (ed). *Ionic liquids: theory, properties, new approaches.* Rijeka: InTech (2011). <http://www.intechopen.com/books/ionic-liquids-theory-properties-new-approaches>. Accessed 28 Feb 2011.
- Ishikawa M, Sugimoto T, Kikuta M, Ishiko E, Kono M. Pure ionic liquid electrolytes compatible with a graphitized carbon negative electrode in rechargeable lithium-ion batteries. *J Power Sources.* 2006;162:658–62.
- Hallett JP, Welton T. Room-temperature ionic liquids: solvents for synthesis and catalysis. *2. Chem Rev.* 2001;11:3508–76.
- Wasserscheid P, Welton T, editors. *Ionic liquids in synthesis.* New York: Wiley-VCH Verlag GmbH; 2008.
- Anderson JL, Armstrong DW. High-stability Ionic liquids. A new class of Stationary phases for gas chromatography. *Anal Chem.* 2003;75:4851–8.
- <https://patents.google.com/patent/US2767119A/en>, grant dated 16 Oct 1956.
- Sunkara GR, Tadavarthi MM, Tadekoru VK, Tadikonda SK, Bezawada SR. Density, refractive index, and speed of sound of the binary mixture of 1-butyl-3-methylimidazolium tetrafluoroborate + *N*-vinyl-2-pyrrolidinone from T = (298.15 to 323.15) K at atmospheric pressure. *J Chem Eng Data.* 2015;60:886–94.
- Suneetha P, Krishna TS, Gowrisankar M, Ravindhranath K, Ramchandran D. Molecular interaction between binary mixtures 1-butyl-3-methyl-imidazolium bis (trifluoromethylsulfonyl) imide with *N*-vinyl-2-pyrrolidinone at different temperatures. *J Chem Thermodyn.* 2017;2017(108):181–92.
- Krishna TS, Narendra K, Sankar MG, Nain AK, Munibhadrayya B. Physicochemical and spectroscopic studies of molecular interactions of 1-butyl-3-methylimidazolium hexafluorophosphate + 2-methoxyethanol or 2-ethoxyethanol binary mixtures at temperatures from 298.15 to 323.15 K. *J Mol Liq.* 2017;227:333–50.
- Scholz E. *Karl Fischer titration.* Berlin: Springer; 1984.
- Dupont J, Consorti CS, Saurez PAZ, de Souza RF. Preparation of 1-butyl-3-methyl imidazolium-based room temperature ionic liquids. *Org Synth.* 2002;79:236.
- Dupont J, Consorti CS, Saurez PAZ, de Souza RF. *Org Synth.* 2004;10:184.
- Danten Y, Cabaco MI, Besnard M. Interaction of water highly diluted in 1-alkyl-3-methyl imidazolium ionic liquids with the PF₆⁻ and BF₄⁻ anions. *J Phys Chem A.* 2009;113:2873.
- Talaty ER, Raja S, Storhaug VJ, Dolle A, Carper WR. Raman and infrared spectra and ab initio calculations of C2-4MIM imidazolium hexafluorophosphate ionic liquids. *J Phys Chem B.* 2004;108:13177.
- Riddick JA, Bunger WB, Sakano TK. *Organic solvents physical properties and methods of purification, vol. II.* 4th ed. New York: Wiley Interscience; 1986.
- Krishna TS, Narendra K, Sankar MG, Nain AK, Munibhadrayya B. Thermodynamic, excess and optical studies on the intermolecular interactions of binary liquid mixtures of imidazolium based ILs. *J Chem Thermodyn.* 2016;2016(98):262–71.
- George J, Sastry NV. Densities, viscosities, speeds of sound, and relative permittivities for water + cyclic amides (2-pyrrolidinone, 1-methyl-2-pyrrolidinone, and 1-vinyl-2-pyrrolidinone) at different temperatures. *J Chem Eng Data.* 2004;49:235–42.
- Gomes de Azevedo R, Esperança JM, Najdanovic-Visak V, Visak ZP, Guedes HJ, Nunes da Ponte M, Rebelo LP. Thermophysical and thermodynamic properties of 1-butyl-3-methylimidazolium tetrafluoroborate and 1-butyl-3-methylimidazolium hexafluorophosphate over an extended pressure range. *J Chem Eng Data.* 2005;50:997–1008.
- Troncoso J, Cerdeirina CA, Sanmamed YA, Romani L, Rebelo LPN. Thermodynamic properties of imidazolium-based ionic liquids: densities, heat capacities, and enthalpies of fusion of [bmim][PF₆] and [bmim][NTf₂]. *J Chem Eng Data.* 2006;51:1856–9.
- Jacquemin J, Ge R, Nancarrow P, Rooney DW, Costa Gomes MF, Padua AA, Hardacre C. Prediction of ionic liquid properties. I. Volumetric properties as a function of temperature at 0.1 MPa. *J Chem Eng Data.* 2008;53:716–26.
- Fan W, Zhou Q, Sun J, Zhang S. Density, excess molar volume, and viscosity for the methyl methacrylate + 1-butyl-3-methylimidazolium hexafluorophosphate ionic liquid binary system at atmospheric pressure. *J Chem Eng Data.* 2009;54:2307–11.
- Zhong Y, Wang H, Diao K. Densities and excess volumes of binary mixtures of the ionic liquid 1-butyl-3-methylimidazolium hexafluorophosphate with aromatic compound at T = (298.15 to 313.15) K. *J Chem Thermodyn.* 2007;39:291–6.
- Pereiro AB, Legido JL, Rodri A. Physical properties of ionic liquids based on 1-alkyl-3-methylimidazolium cation and hexafluorophosphate as anion and temperature dependence. *J Chem Thermodyn.* 2007;39:1168–75.
- Geng Y, Chen S, Wang T, Yu D, Peng C, Liu H, Hu Y. Density, viscosity and electrical conductivity of 1-butyl-3-methylimidazolium hexafluorophosphate + monoethanolamine and + *N,N*-dimethylethanolamine. *J Mol Liq.* 2008;143:100–8.
- Pal A, Kumar B. Volumetric, acoustic and spectroscopic studies for binary mixtures of ionic liquid (1-butyl-3-methylimidazolium

- hexafluorophosphate) with alkoxyalkanols at $T = (288.15 \text{ to } 318.15) \text{ K}$. *J Mol Liq.* 2011;163:128–34.
28. Suneetha P, Krishna TS, Gowrisankar M, Ramachandran D. Volumetric, acoustic and spectroscopic study of 1-butyl-3-methylimidazolium trifluoromethanesulfonate with alkoxyalkanols at different temperatures. *J Mol Liq.* 2017;238:170–83.
 29. Krishna TS, Nain AK, Chentilnath S, Punyaseshudu D, Munibhadrayya B. Densities, ultrasonic speeds, refractive indices, excess and partial molar properties of binary mixtures of imidazolium based ionic liquid with pyrrolidin-2-one at temperatures from 298.15 K. *J Chem Thermodyn.* 2016;101:103–14.
 30. Douheret G, Davis MI, Reis JCR, Blandamer MJ. Isentropic compressibilities-experimental origin and the quest for their rigorous estimation in thermodynamically ideal liquid mixtures. *Chem Phys Chem.* 2001;2:148–61.
 31. Douheret G, Davis MI, Reis JCR. Excess isentropic compressibilities and excess ultrasound speeds in binary and ternary liquid mixtures. *Fluid Phase Equilib.* 2005;231:246–9.
 32. Benson GC, Kiyohara O. Evaluation of excess isentropic compressibilities and isochoric heat capacities. *J Chem Thermodyn.* 1979;11:1061–4.
 33. Srinivasu JV, Krishna TS, Narendra K, SrinivasaRao G, SubbaRao B. Elucidation of H-bond and molecular interactions of 1,4-butanediol with cresols: acoustic and volumetric data. *J Mol Liq.* 2017;236:27–37.
 34. Cerdeirina CA, Tovar CA, Lez-Salgado DG, Carballo E, Romanoa L. Isobaric thermal expansivity and thermophysical characterization of liquids and liquid mixtures. *Phys Chem Chem Phys.* 2001;3:5230–6.
 35. Brocos P, Pineiro A, Bravo R, Amigo A. Refractive indices, molar volumes and molar refractions of binary liquid mixtures: concepts and correlations. *Phys Chem Chem Phys.* 2003;5:550–7.
 36. Redlich O, Kister AT. Algebraic representation of thermodynamic properties and the classification of solutions. *Ind Eng Chem.* 1948;40:345–8.
 37. Iloukhani H, Ghorbani R. Volumetric properties of *N,N*-dimethylformamide with 1, 2-alkanediols at 20 °C. *J Sol Chem.* 1998;27(2):141–9.
 38. Davis MI, Douheret G, Reis JCR, Blandamer MJ. Apparent and partial ideal molar isentropic compressibilities of binary liquid mixtures. *Phys Chem Chem Phys.* 2001;3:4555–9.
 39. Krishna TS, Raju KTSS, Gowrisankar M, Nain AK, Munibhadrayya B. Volumetric, ultrasonic and spectroscopic studies of molecular interactions in binary mixtures of 1-butyl-3-methylimidazolium hexafluorophosphate with 2-propoxyethanol at temperatures from 298.15 to 323.15 K. *J Mol Liq.* 2016;216:484–95.
 40. Ali A, Nain AK. Ultrasonic and volumetric study of binary mixtures of benzyl alcohol with amides. *Bull Chem Soc Jpn.* 2002;75:681–7.
 41. Assarsson P, Eirich FR. Properties of amides in aqueous solution. I. Viscosity and density changes of amide-water systems. An analysis of volume deficiencies of mixtures based on molecular size differences (mixing of hard spheres). *J Phys Chem.* 1968;72:2710–9.
 42. Zafarani-Moattar MT, Shekaari H. Volumetric and speed of sound of ionic liquid, 1-butyl-3-methylimidazolium hexafluorophosphate with acetonitrile and methanol at $T = (298.15 \text{ to } 318.15) \text{ K}$. *J Chem Eng Data.* 2005;50:1694–9.
 43. Wang J, Zhu A, Zhao Y, Zhuo K. Excess molar volumes and excess logarithm viscosities for binary mixtures of the ionic liquid 1-butyl-3-methylimidazolium hexafluorophosphate with some organic compounds. *J Solution Chem.* 2005;34:585–96.
 44. Reddy PM, Venkatesu P. Densities and ultrasonic studies for binary mixtures of tetrahydrofuran with chlorobenzenes, chlorotoluenes and nitrotoluenes at 298.15 K. *Fluid Phase Equilib.* 2011;310:74–81.
 45. Hunt PA, Kirchner B, Welton T. Characterising the electronic structure of ionic liquids: an examination of the 1-butyl-3-methylimidazolium chloride ion pair. *J Chem Eur.* 2006;12:6762–75.
 46. Aggarwal A, Lancaster NL, Sethi AR, Welton T. The role of hydrogen bonding in controlling the selectivity of Diels-Alder reactions in room-temperature ionic liquids. *Green Chem.* 2002;4:517–20.
 47. Znamenskiy V, Kobrak MN. Molecular dynamics study of polarity in room-temperature ionic liquids. *J Phys Chem B.* 2004;2004(108):1072–9.
 48. Crosthwaite JM, Aki SN, Maginn EJ, Brennecke JF. Liquid phase behavior of imidazolium-based ionic liquids with alcohols. *J Phys Chem B.* 2004;2004(108):5113–9.
 49. Kawaizumi F, Ohno M, Miyahara Y. Ultrasonic and volumetric investigation of aqueous solutions of amides. *Bull Chem Soc Jpn.* 1977;50:2229–36.
 50. Prakash O, Sinha S. Ultrasonic studies in binary mixtures of tetrahydrofuran with formamide, methyl formamide, dimethyl formamide and 2-methyl pyridine. *Acustica.* 1984;54:223–5.
 51. Pineiro A, Brocos P, Amigo A, Pintos M, Bravo R. Prediction of excess volumes and excess surface tensions from experimental refractive indices. *Phys Chem Liq.* 2000;38:251–60.
 52. Hall L. The origin of ultrasonic absorption in water. *Phys Rev.* 1948;73:775–84.
 53. Hawrylak B, Gracie K, Palepu R. Thermodynamic properties of binary mixtures of butanediols with water. *J Solution Chem.* 1998;27:17–31.
 54. Cipiciani A, Onori G, Savelli G. Structural properties of water-ethanol mixtures: a correlation with the formation of micellar aggregates. *Chem Phys Lett.* 1988;143:505–9.
 55. Tariq M, Forte PAS, Gomes MC, Lopes JC, Rebelo LPN. Densities and refractive indices of imidazolium-and phosphonium-based ionic liquids: effect of temperature, alkyl chain length, and anion. *J Chem Thermodyn.* 2009;41:790–8.
 56. Iglesias-Otero MA, Troncoso J, Carballo E, Román L. Density and refractive index in mixtures of ionic liquids and organic solvents: correlations and predictions. *J Chem Thermodyn.* 2008;2008(40):949–56.
 57. Mehra R. Application of refractive index mixing rules in binary systems of hexadecane and heptadecane with n-alkanols at different temperatures. *Proc Indian Acad Sci (Chem Sci).* 2003;115:147–54.